Report

Current Biology

Tropomyosin Promotes Lamellipodial Persistence by Collaborating with Arp2/3 at the Leading Edge

Graphical Abstract

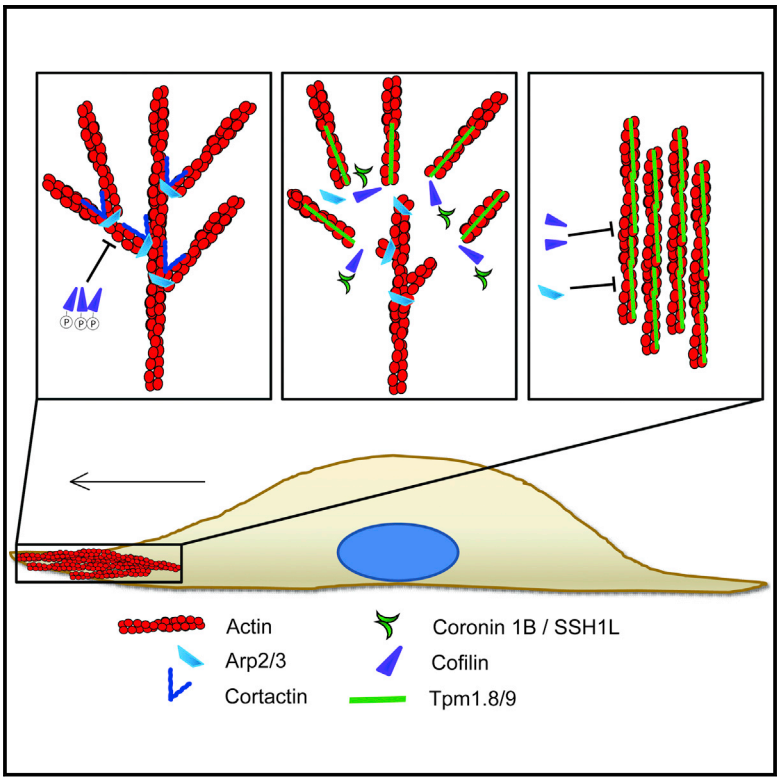

Authors

Simon Brayford, Nicole S. Bryce, Galina Schevzov, Elizabeth M. Haynes, James E. Bear, Edna C. Hardeman, Peter W. Gunning

Correspondence

p.gunning@unsw.edu.au

In Brief

Two molecularly distinct actin filament networks occupy the lamellipodium of motile cells. Brayford et al. show that the tropomyosin isoforms Tpm1.8/9 are highly enriched in the lamellipodium and define a specific subset of actin filaments, which together with coronin 1B are responsible for enhancing the persistence of lamellipodial protrusions.

Highlights

- Tropomyosins Tpm1.8/9 are enriched in the lamellipodium alongside Arp2/3
- Tpm1.8/9 knockdown enhances Arp2/3 activity
- Tpm1.8/9 promote lamellipodial persistence and cell motility
- Coronin 1B and cofilin cooperate to generate Tpm1.8/9-actin filaments

Brayford et al., 2016, Current Biology *26*, 1312–1318
May 23, 2016
http://dx.doi.org/10.1016/j.cub.2016.03.028

CellPress

CellPress

Current Biology
Report

Tropomyosin Promotes Lamellipodial Persistence by Collaborating with Arp2/3 at the Leading Edge

Simon Brayford,[1] Nicole S. Bryce,[1] Galina Schevzov,[1] Elizabeth M. Haynes,[2] James E. Bear,[2] Edna C. Hardeman,[3] and Peter W. Gunning[1,*]

[1]Oncology Research Unit, School of Medical Sciences, UNSW Australia, Sydney, NSW 2052, Australia
[2]Department of Cell and Developmental Biology, University of North Carolina, Chapel Hill, NC 27599-3280, USA
[3]Cellular and Genetic Medicine Unit, School of Medical Sciences, UNSW Australia, Sydney, NSW 2052, Australia
*Correspondence: p.gunning@unsw.edu.au
http://dx.doi.org/10.1016/j.cub.2016.03.028

SUMMARY

At the leading edge of migrating cells, protrusion of the lamellipodium is driven by Arp2/3-mediated polymerization of actin filaments [1]. This dense, branched actin network is promoted and stabilized by cortactin [2, 3]. In order to drive filament turnover, Arp2/3 networks are remodeled by proteins such as GMF, which blocks the actin-Arp2/3 interaction [4, 5], and coronin 1B, which acts by directing SSH1L to the lamellipodium where it activates the actin-severing protein cofilin [6, 7]. It has been shown in vitro that cofilin-mediated severing of Arp2/3 actin networks results in the generation of new pointed ends to which the actin-stabilizing protein tropomyosin (Tpm) can bind [8]. The presence of Tpm in lamellipodia, however, is disputed in the literature [9–19]. Here, we report that the Tpm isoforms 1.8/9 are enriched in the lamellipodium of fibroblasts as detected with a novel isoform-specific monoclonal antibody. RNAi-mediated silencing of Tpm1.8/9 led to an increase of Arp2/3 accumulation at the cell periphery and a decrease in the persistence of lamellipodia and cell motility, a phenotype consistent with cortactin- and coronin 1B-deficient cells [2, 7]. In the absence of coronin 1B or cofilin, Tpm1.8/9 protein levels are reduced while, conversely, inhibition of Arp2/3 with CK666 leads to an increase in Tpm1.8/9 protein. These findings establish a novel regulatory mechanism within the lamellipodium whereby Tpm collaborates with Arp2/3 to promote lamellipodial-based cell migration.

RESULTS AND DISCUSSION

The precise localization of Tpm at the leading edge of cells has been controversial with studies reporting the absence of Tpms from lamellipodia [9–11, 13], and others reporting their presence at or near lamellipodia [16–19]. These opposing observations are partly due to the lack of appropriate reagents to detect the Tpms. Here, we report the characterization of a novel monoclonal antibody (α/1b) generated by two overlapping peptides spanning the entire exon 1b of the *Tpm1* gene as the immunogen (Figure 1A). A panel of recombinant Tpm proteins comprising isoforms representing all four *Tpm* genes was probed with the α/1b antibody. It preferentially detects isoforms Tpm1.8 and Tpm1.9 with minor cross reactivity with Tpm2.1 (Figure 1B). Tpm1.8/9 share a similar amino-terminal exon/intron structure with Tpm1.12 [19], an isoform found at the leading edge of neuronal cells [17]. The spatial distribution of Tpm1.8/9 was assessed in mouse embryonic fibroblasts (MEFs) that display characteristic lamellipodia [20]. MEFs were co-stained with α/1b and CG1 (an antibody specific for Tpm2.1 [19]) in order to demonstrate that lamellipodial staining in these cells is due to the presence of Tpm1.8/9 rather than Tpm2.1, which is more prominent in stress fibers [19, 21, 22]) (Figures 1C and 1D) (see also Figures S1 and S2). MEFs were also co-stained with anti-cortactin and anti-Arp2 to demonstrate that both of these proteins are present in the lamellipodium (Figure 1E), as well as with α/1b and anti-Arp2 (Figure 1F). Finally, 3 × 3-μm enlargements (Figure 1G) of regions along the leading edge (indicated in the merge panel of Figure 1F) reveal that, although both are present in the lamellipodium, Tpm1.8/9 (red) and Arp2 (green) do not overlap significantly. Co-localization was quantitated using Pearson's coefficient (Figure 1G), showing that, compared to a cortactin control, Tpm1.8/9 and Arp2 display a significantly lower level of co-localization (R), suggesting that Tpm1.8/9 and Arp2/3 associate with different populations of actin filaments within the lamellipodium. This is supported by in vitro studies that showed that binding of the Arp2/3 complex to actin filaments is inhibited by Tpm1.9 [10], but interestingly, not the related Tpm1.12 [17, 23].

Due to the biochemical incompatibility of Arp2/3 and most Tpms, early reports suggested that they were spatially segregated [10, 11]. It has also been proposed that persistent advancement of the cell relies on the underlying lamella [12, 24], which is supported by observations that cell migration is possible without a lamellipodium [13] and Arp2/3 is dispensable for chemotaxis [25]. To investigate the potential role of Tpm1.8/9 in regulating Arp2/3 within the lamellipodium, we designed a small interfering RNA (siRNA) to target exon 1b of the mouse *Tpm1* gene. Western blot analysis of MEF lysates 48 hr post-transfection shows successful knockdown of Tpm1.8/9 protein (Figure 2A) without impacting other Tpm isoforms (Figure S3). Cells were submitted to a random migration assay, which revealed that Tpm1.8/9 siRNA-treated cells exhibited a significant reduction in whole-cell velocity (Figure 2B). Leading edge dynamics was evaluated by generating kymographs of

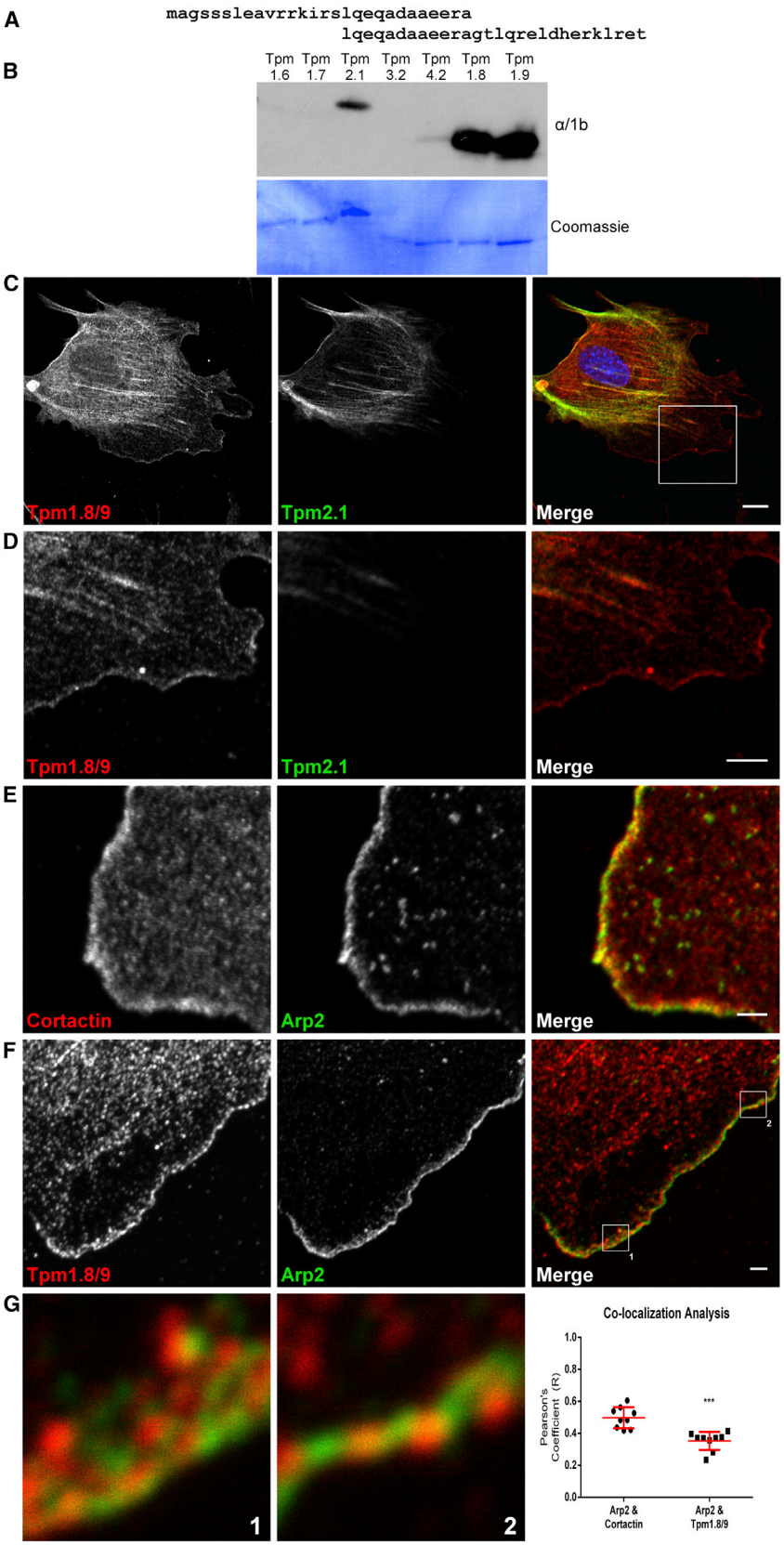

Figure 1. The Tpm Isoforms 1.8/9 Are Enriched in the Lamellipodium of Fibroblasts as Detected with a Novel Isoform-Specific Monoclonal Antibody

(A) Peptides that span the entire exon 1b of the *Tpm1* gene were used as the immunogen to generate the rat α/1b monoclonal antibody.

(B) Western blot of recombinant Tpm isoforms showing isoform specificity of the α/1b antibody for Tpm1.8 and Tpm1.9 with minor cross-reactivity with Tpm2.1.

(C) Representative confocal image of a MEF cell co-stained for Tpm1.8/9 and Tpm2.1, demonstrating that only Tpm1.8/9 are present in the lamellipodium. Merged image shows Tpm1.8/9 in red, Tpm2.1 in green and nucleus stain with DAPI (blue). Scale bar, 10 μm. See also Figure S1.

(D) 30 × 30-μm enlargement of the boxed region in (C) (merge) showing, in detail, the presence of Tpm1.8/9 and absence of Tpm2.1 from the lamellipodium. Scale bar, 5 μm.

(E) 5× magnification of the lamellipodium of a MEF cell co-stained for cortactin and Arp2, used as a control to demonstrate that both of these proteins occupy the lamellipodium. Merged image shows cortactin in red and Arp2 in green. Scale bar, 2 μm.

(F) 3× magnification of the lamellipodium of a MEF cell co-stained for Tpm1.8/9 and Arp2 to demonstrate that both of these proteins occupy the lamellipodium. Merged image shows Tpm1.8/9 in red and Arp2 in green. Scale bar, 2 μm.

(G) 3 × 3-μm enlargements of the regions shown in the merge panel from (E), showing that, although both present in the lamellipodium, Tpm1.8/9 (red) and Arp2 (green) do not strongly overlap. This is demonstrated quantitatively by co-localization analysis of the images by Pearson's coefficient, where compared to cortactin control (individual zooms not shown), Tpm1.8/9 and Arp2 display a significantly lower level of co-localization (R). Error bars ± SEM; n = 9; ***$p < 0.001$; Student's t test.

See also Figures S1 and S2.

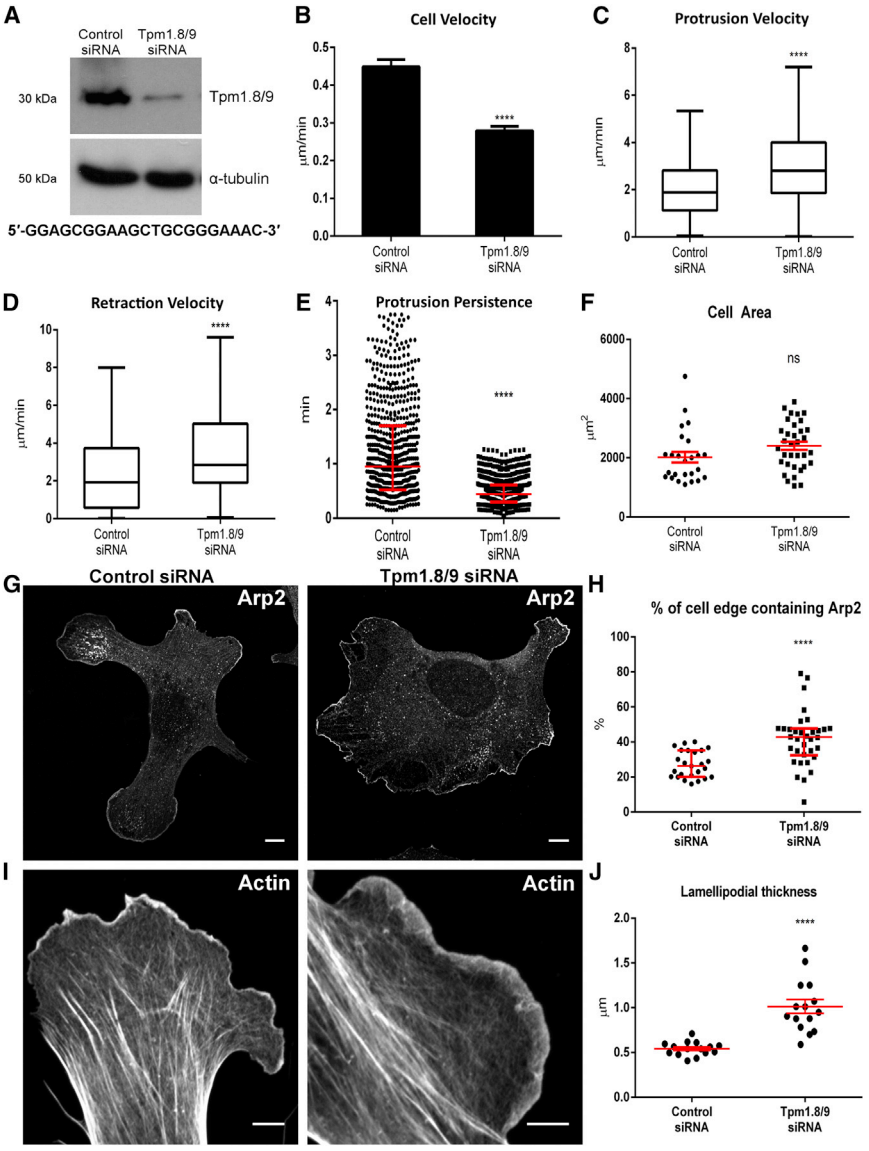

Figure 2. RNAi-Mediated Silencing of Tpm1.8/9 Results in Reduced Cell Speed and Lamellipodial Persistence and Leads to an Increase of Arp2/3 Accumulation at the Cell Periphery

(A) Western blot showing Tpm1.8/9 expression in MEFs 48 hr post-transfection with either control (non-silencing) or Tpm1.8/9 siRNA. α-tubulin was used as a loading control. Target sequence shown below blot.

(B) Histogram showing average (control, n = 79 cells; Tpm1.8/9 siRNA, n = 74 cells) cell velocity. Error bars, SEM; n = 4, ****p < 0.0001; Student's t test.

(C and D) Quantitation of kymographs (control, n = 228 kymographs generated for 30 cells; Tpm1.8/9 siRNA, n = 181 kymographs generated for 23 cells) showing the velocity of protrusions (C) and retractions (D). For Tukey boxplots, whiskers indicate maximum and minimum values within 1.5 interquartile range (IQR), the box represents the 25th–75th quartile, and the line indicates the median. n = 4; ****p < 0.0001; Student's t test.

(E) Quantitation of kymographs showing protrusion persistence in Tpm1.8/9-treated cells compared to control siRNA-treated cells. Error bars ± SEM; control siRNA, n = 228 kymographs generated for 30 cells; Tpm1.8/9 siRNA, n = 181 kymographs generated for 23 cells; ****p < 0.0001; Student's t test.

(F) Quantitation of image analysis showing no significant difference in cell area in control siRNA compared to Tpm1.8/9 siRNA-treated cells. Error bars ± SEM; n = 25; ns, not statistically significant; Student's t test.

(G) MEFs stained for Arp2, 48 hr post-transfection with either control (left) or Tpm1.8/9 siRNA (right). Scale bars, 10 μm.

(H) Quantitation of image analysis showing percentage of cell edge containing Arp2 is significantly increased in the knockdowns. Error bars ± SEM; n = 25; ****p < 0.0001; Student's t test.

(I) MEFs stained with phalloidin, 48 hr post-transfection with either control (left, 2.0× magnification) or Tpm1.8/9 siRNA (right, 2.6× magnification). Scale bars, 5 μm.

(J) Quantitation of image analysis showing lamellipodial thickness is significantly increased in Tpm1.8/9 knockdown cells. Error bars ± SEM; n = 15; ****p < 0.0001; Student's t test.

See also Figure S3.

active lamellipodia taken from 10 min live differential interference contrast (DIC) movies of control or Tpm1.8/9 knockdown MEFs. Analysis of the kymographs revealed that, while protrusion velocity (Figure 2C) and retraction velocity (Figure 2D) were both increased as a result of Tpm1.8/9 knockdown, protrusion persistence, a measure of lamellipodial stability, was significantly reduced in Tpm1.8/9 siRNA-treated cells (Figure 2E). Since persistent advancement of the lamellipodium is largely driven by Arp2/3 activity, and Arp2/3 and Tpm1.8/9 appear to associate with different actin filament populations (Figure 1G), we postulated that Tpm1.8/9 may have an antagonistic effect on the binding of Arp2/3 to actin filaments within the lamellipodium, a property of Tpm1.9 in vitro [10]. To test this, we measured the percentage of the cell edge that contains Arp2 relative to cell area in control and Tpm1.8/9 knockdown cells (Figure 2G). While we observed no significant change in cell area (Figure 2F), we saw a significant increase in the percentage of the cell edge that contains Arp2 in the Tpm1.8/9 knockdown cells compared to control (Figure 2H), suggesting that knockdown of Tpm1.8/9 results in an increased ability of the Arp2/3 complex to bind to actin filaments and spread along the cell periphery. Finally, as Arp2/3 activity generates a dense, branched actin network, we hypothesized that its increased activity, due to reduced inhibition from Tpm1.8/9, should also lead to a thicker lamellipodium due to an increased abundance of branched, filamentous actin (F-actin) at the leading edge. The lamellipodium is clearly identifiable as an F-actin-rich band, as probed by phalloidin

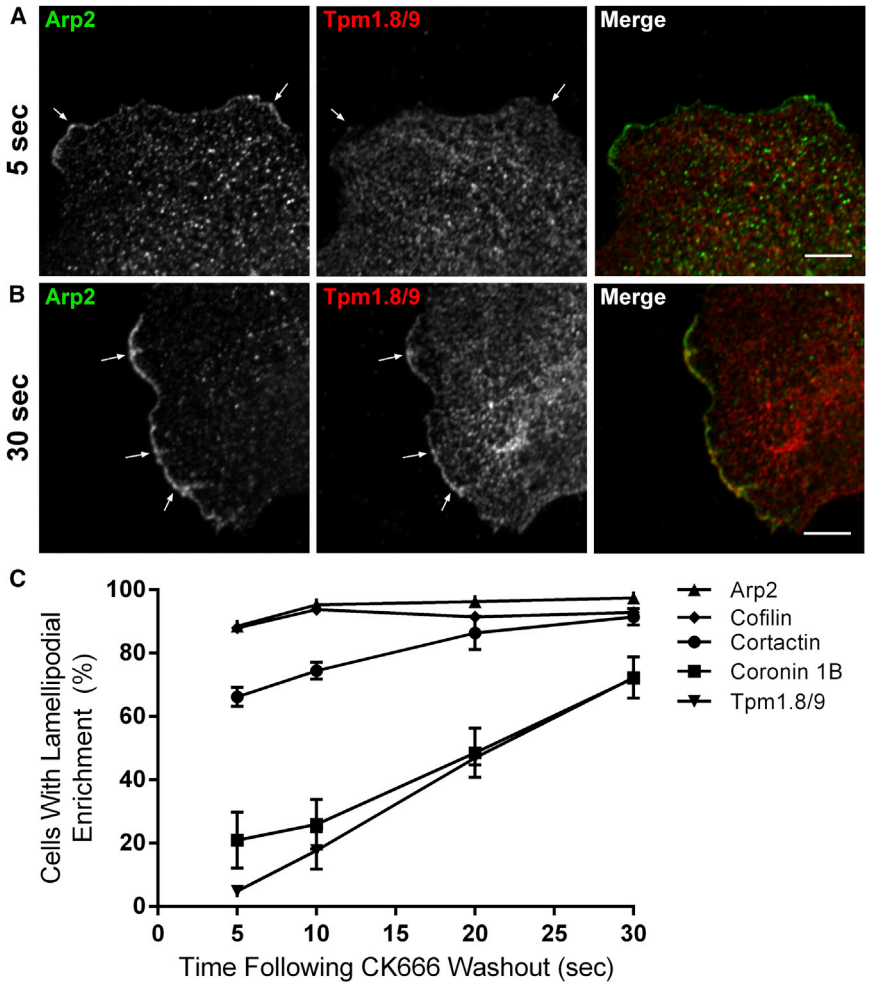

Figure 3. Sequence of Appearance of Other Actin Binding Proteins following Activation of the Arp2/3 Complex

Cells were treated with the Arp2/3 inhibitor CK666 at 150 μM for 3 hr, and the inhibitor was then washed out. Cells were fixed at 5, 10, 20, or 30 s.

(A) Representative confocal image of a newly formed lamellipodium in a MEF cell (3× magnification), co-stained for Arp2 (green) and Tpm1.8/9 (red) at 5 s following washout of CK666. Scale bar, 5 μm.

(B) Representative confocal image of a newly formed lamellipodium in a MEF cell (3× magnification), co-stained for Arp2 (green) and Tpm1.8/9 (red) at 30 s following washout of CK666. Scale bar, 5 μm.

(C) Quantitation shown as a percentage of cells displaying lamellipodial enrichment of the relevant protein at the various time points following drug washout; error bars ± SEM; n > 100 cells per antibody per time point. n = 3.

in fibroblasts [26]. We measured the width of the lamellipodium in control and Tpm1.8/9 knockdown cells (Figure 2I). Analysis of 15 cells from each group revealed that lamellipodia in the Tpm1.8/9 knockdown cells were, on average, significantly thicker than those in the control group (Figure 2J).

There is controversy in the literature about the organization of the actin network at the leading edge. Some studies have reported the existence of two spatially segregated zones composed of Arp2/3-branched filaments at the cell edge, and unbranched filaments immediately proximal to this zone [1, 9, 27–29]. Others have stated that these overlap and that both branched and unbranched filaments are present at the very leading edge [30–32]. The formation of a linear array of actin filaments at the leading edge would need to be governed by a precise sequence of appearance of other actin binding proteins following activation of the Arp2/3 complex. Coronin 1B and cofilin have been shown to cooperate to drive the turnover of branched filaments to establish a new network of F-actin [3, 6–8]. To determine whether Tpm1.8/9-containing actin filaments derive from the formation of this F-actin network, the Arp2/3 inhibitor CK666 was used to abolish the lamellipodium. Upon washout of the inhibitor, Arp2/3 activity is rapidly restored and formation of new lamellipodia can be synchronized [33, 34]. We found that, after 5 s of washout of the inhibitor, Arp2 staining can be seen at the very tips of newly formed lamellipodia (Figure 3A). This is consistent with the well-established role of Arp2/3 in the initiation of lamellipodia [13, 23, 25, 35]. Strikingly, Tpm1.8/9 is absent from these structures at this early time point. However, after 30 s, some enrichment of Tpm1.8/9 is clearly visible at the periphery of cells (Figure 3B). We also examined the time course of appearance of other actin binding proteins and found that cortactin is also rapidly recruited following the re-activation of Arp2/3, although not to the same extent as Arp2/3 (Figure 3C). This is also consistent with the role of cortactin in the stabilization of Arp2/3-nucleated filaments at the leading edge [2, 3]. In contrast, significantly fewer cells displayed coronin 1B enrichment at the leading edge at 5 or 10 s after CK666 washout, with enrichment seen in the majority of cells after 30 s of washout. Collectively, these data indicate that coronin 1B and Tpm1.8/9, while not essential for initiation of lamellipodial protrusion, may play a role in the maintenance and persistence of lamellipodia by generating and stabilizing the F-actin network. Finally cofilin, which is present fairly homogenously throughout the cell, including the lamellipodium, in both migrating and non-migrating fibroblasts [26], was enriched at the very earliest of time points closely following that of Arp2/3. Cofilin is activated via dephosphorylation by protein phosphatase slingshot homolog 1 (SSH1L), which is directed to the lamellipodium by coronin 1B [7]. We postulate that, although cofilin is present in early lamellipodia, it is not until the later recruitment of coronin 1B/SSH1L that cofilin is activated and begins severing the Arp2/3 network, as has been described in a cell-free system [8].

These findings raise an important question, how can multiple actin filament populations co-exist in the same cellular region yet be differentially regulated [17]? It has recently been shown in vitro that severing of Arp2/3-generated networks by cofilin results in the generation of new pointed ends to which the

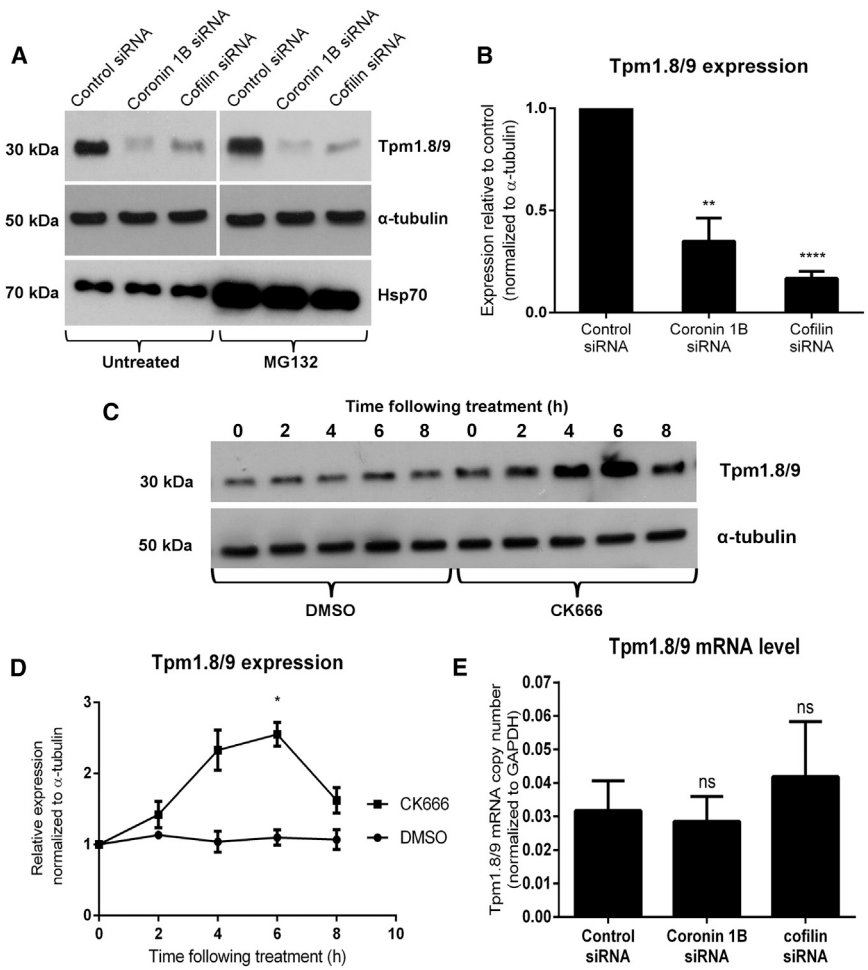

Figure 4. In the Absence of Coronin 1B or Cofilin, Tpm1.8/9 Protein Levels Are Reduced While, Conversely, Inhibition of Arp2/3 with CK666 Leads to an Increase in Tpm1.8/9 Protein

(A) Western blot showing degradation of Tpm1.8/9 protein following siRNA knockdown of either coronin 1B or cofilin compared to control siRNA (top panel, left) with α-tubulin as a loading control (middle panel). Treatment with proteasome inhibitor MG132 does not restore Tpm1.8/9 protein levels (top panel, right). The same lysates from the upper panels were run together on a separate gel and probed for Hsp70 as a positive control to demonstrate successful inhibition of the proteasome (lower panel, right) compared to lysates from untreated cells (lower panel, left).

(B) Quantitation of western blots showing a significant reduction in Tpm1.8/9 protein levels (normalized to α-tubulin) following siRNA knockdown of coronin 1B or cofilin compared to control; error bars, SEM; n = 3; $^{**}p < 0.01$, $^{****}p < 0.0001$; Student's t test.

(C) Western blot showing Tpm1.8/9 protein levels at 2-hr time points following CK666 treatment compared to DMSO vehicle control. α-tubulin was used as a loading control.

(D) Quantitation of western blots in (C) showing an increase in Tpm1.8/9 protein levels (normalized to α-tubulin) post-CK666 treatment with a statistically significant increase at 6 hr post-treatment. Error bars ± SEM; n = 3; $^{*}p < 0.05$; Student's t test.

(E) qPCR analysis of Tpm1.8/9 mRNA taken from cDNA generated from either control, coronin 1B, or cofilin siRNA-treated cells; error bars, SEM; n = 2; ns, not statistically significant; Student's t test.

See also Figures S2 and S4.

Drosophila-derived Tpm, Tm1A, preferentially binds, generating two sets of actin filaments. One is Tpm coated and the other Tpm free that is competent to bind Arp2/3. They can be stably maintained in vitro because they are insulated from each another [8]. These findings point toward a potential mechanism of how branched actin filaments may be re-modeled in cells to include Tpm. Recent experiments indicate the importance of building multiple actin filament types in the same location to generate functional outcomes [36, 37]. Studies in a variety of systems support that Tpm isoforms are used to specify the functional and molecular properties of actin filaments to allow the collaboration of different filament populations within the cell [38]. By a mechanism that is not yet fully understood, Tpm isoforms display extensive sorting, both at a tissue and intracellular level resulting in spatially distinct actin filament populations [22, 39]. Because of the co-recruitment of Tpm1.8/9 and coronin 1B in newly formed lamellipodia, we postulated that coronin 1B and/or active cofilin may be required for Tpm1.8/9 targeting to lamellipodial actin filaments. To test this, we used siRNA sequences to knockdown coronin 1B or its downstream effector cofilin and examined Tpm1.8/9 localization using the α/1b antibody. We observed that significantly fewer cells displayed lamellipodial enrichment of Tpm1.8/9 in the coronin 1B (24.6% ± 2.0%, $p < 0.0001$) and cofilin (16.0% ± 3.3%, $p < 0.0001$) siRNA knockdown cells compared to control cells (71.3% ± 1.3%) (images not shown). We hypothesized that the lack of Tpm1.8/9 at the leading edge following the knockdown of coronin 1B or cofilin could potentially be as a result of protein degradation. Western blots of siRNA-treated cell lysates demonstrate a significant reduction in the overall levels of Tpm1.8/9 (Figures 4A, upper panel, and 4B). As no significant change was observed in the mRNA levels for Tpm1.8/9 as revealed by qPCR (Figure 4E), this effect is likely due to Tpm1.8/9 protein being degraded when it cannot bind as effectively to actin filaments in the lamellipodium. To investigate whether Tpm1.8/9 was being degraded by the 26S proteasome, the proteasome inhibitor MG132 was used. Cells transfected with Coronin 1B or cofilin siRNA were treated with 20 μM MG132 for 6 hr. Protein lysates for treated and untreated cells were separated by SDS-PAGE, and blots were probed with the α/1b antibody. The same lysates were later run on a separate gel alongside non-inhibitor-treated lysates and probed for Hsp70, a chaperone that is known to be degraded by the 26S proteasome. As expected, the MG132-treated samples showed increased levels of Hsp70 compared to untreated samples (Figure 4A, lower panel). There was no apparent restoration of Tpm1.8/9 protein levels following MG132 treatment (Figure 4A, upper panel) suggesting Tpm1.8/9 is not degraded by the proteasome. In contrast to the result of Coronin 1B/cofilin

knockdown, knockdown of cortactin had no significant impact on the localization ($p = 0.7828$) or protein level ($p = 0.0785$) of Tpm1.8/9 (Figure S4). Finally, we examined the effect of CK666 on Tpm1.8/9 protein levels using a time-course assay and found that after 6-hr exposure to the Arp2/3 inhibitor, Tpm1.8/9 levels were significantly increased compared to DMSO control (Figures 4C and 4D). Despite an increase in protein level, Tpm1.8/9 is not redistributed to other structures such as stress fibers (Figure S2D). This result further indicates a regulatory relationship between Arp2/3 and Tpm1.8/9, whereby, if Tpm1.8/9 is silenced, Arp2/3 activity increases (Figures 2H and 2J), and, conversely, if Arp2/3 is inhibited by CK666, Tpm1.8/9 expression is transiently increased (Figures 4C and 4D). This effect is supported by the results outlined in Figure 3, whereby under CK666 inhibition, even though expression is upregulated, Tpm1.8/9 do not have access to the leading edge until Arp2/3 activity is restored and coronin 1B/cofilin remodeling can take place.

The findings of this study may provide a solution to the controversy found in the literature and offer a novel mechanism of how Tpm and Arp2/3 collaborate at the leading edge. At the advancing cell edge, coronin 1B and cofilin coordinate the transition between a network of non-Tpm-containing Arp2/3-branched filaments and a second, Tpm-containing network of linear filaments by generating exposed pointed ends, which become coated with Tpm1.8/9. This provides the stability needed to enhance persistence through the subsequent promotion of substratum adhesions. In the absence of coronin 1B, cofilin is not activated and fewer free pointed ends to which Tpm can bind are created. Tpm may be subsequently degraded and therefore depleted from the leading edge, an observation also seen following the knockdown of cofilin. As a result of reduced Tpm levels, the presence of more stable, unbranched filaments is diminished and lamellipodial persistence is impaired. In conclusion, the tropomyosin isoforms Tpm1.8/9 are specifically recruited to the leading edge of migrating cells where they promote the transition from a branched actin network to a more stable actin network in order to achieve a persistent state of lamellipodial protrusion.

SUPPLEMENTAL INFORMATION

Supplemental Information includes four figures and Supplemental Experimental Procedures and can be found with this article online at http://dx.doi.org/10.1016/j.cub.2016.03.028.

AUTHOR CONTRIBUTIONS

Conceptualization, S.B. and P.W.G.; Methodology, S.B., E.M.H., and J.E.B.; Investigation, S.B.; Formal Analysis, S.B. and N.S.B.; Writing – Original Draft, S.B.; Writing – Review & Editing, G.S., N.S.B., E.C.H., and P.W.G.; Funding Acquisition and Supervision, G.S., J.E.B., E.C.H., and P.W.G.

ACKNOWLEDGMENTS

This work was supported by project grant APP1004175 from the Australian National Health and Medical Research Council (NHMRC) (P.W.G., G.S., and E.C.H.) and funding from The Kids Cancer Project. S.B. is the recipient of an Australian Postgraduate Award and is supported by the Translational Cancer Research Network (TCRN), Australia. P.W.G. is a non-executive Director of Novogen Ltd., a company that is developing anti-tropomyosin drugs for the treatment of childhood and adult cancer.

Received: August 26, 2015
Revised: February 2, 2016
Accepted: March 10, 2016
Published: April 21, 2016

REFERENCES

1. Pollard, T.D., and Borisy, G.G. (2003). Cellular motility driven by assembly and disassembly of actin filaments. Cell *112*, 453–465.
2. Bryce, N.S., Clark, E.S., Leysath, J.L., Currie, J.D., Webb, D.J., and Weaver, A.M. (2005). Cortactin promotes cell motility by enhancing lamellipodial persistence. Curr. Biol. *15*, 1276–1285.
3. Weaver, A.M., Karginov, A.V., Kinley, A.W., Weed, S.A., Li, Y., Parsons, J.T., and Cooper, J.A. (2001). Cortactin promotes and stabilizes Arp2/3-induced actin filament network formation. Curr. Biol. *11*, 370–374.
4. Poukkula, M., Hakala, M., Pentinmikko, N., Sweeney, M.O., Jansen, S., Mattila, J., Hietakangas, V., Goode, B.L., and Lappalainen, P. (2014). GMF promotes leading-edge dynamics and collective cell migration in vivo. Curr. Biol. *24*, 2533–2540.
5. Haynes, E.M., Asokan, S.B., King, S.J., Johnson, H.E., Haugh, J.M., and Bear, J.E. (2015). GMFβ controls branched actin content and lamellipodial retraction in fibroblasts. J. Cell Biol. *209*, 803–812.
6. Cai, L., Makhov, A.M., Schafer, D.A., and Bear, J.E. (2008). Coronin 1Bantagonizes cortactin and remodels Arp2/3-containing actin branches in lamellipodia. Cell *134*, 828–842.
7. Cai, L., Marshall, T.W., Uetrecht, A.C., Schafer, D.A., and Bear, J.E. (2007). Coronin 1B coordinates Arp2/3 complex and cofilin activities at the leading edge. Cell *128*, 915–929.
8. Hsiao, J.Y., Goins, L.M., Petek, N.A., and Mullins, R.D. (2015). Arp2/3 complex and cofilin modulate binding of tropomyosin to branched actin networks. Curr. Biol. *25*, 1573–1582.
9. Iwasa, J.H., and Mullins, R.D. (2007). Spatial and temporal relationships between actin-filament nucleation, capping, and disassembly. Curr. Biol. *17*, 395–406.
10. Blanchoin, L., Pollard, T.D., and Hitchcock-DeGregori, S.E. (2001). Inhibition of the Arp2/3 complex-nucleated actin polymerization and branch formation by tropomyosin. Curr. Biol. *11*, 1300–1304.
11. DesMarais, V., Ichetovkin, I., Condeelis, J., and Hitchcock-DeGregori, S.E. (2002). Spatial regulation of actin dynamics: a tropomyosin-free, actin-rich compartment at the leading edge. J. Cell Sci. *115*, 4649–4660.
12. Ponti, A., Machacek, M., Gupton, S.L., Waterman-Storer, C.M., and Danuser, G. (2004). Two distinct actin networks drive the protrusion of migrating cells. Science *305*, 1782–1786.
13. Gupton, S.L., Anderson, K.L., Kole, T.P., Fischer, R.S., Ponti, A., Hitchcock-DeGregori, S.E., Danuser, G., Fowler, V.M., Wirtz, D., Hanein, D., and Waterman-Storer, C.M. (2005). Cell migration without a lamellipodium: translation of actin dynamics into cell movement mediated by tropomyosin. J. Cell Biol. *168*, 619–631.
14. Skau, C.T., Plotnikov, S.V., Doyle, A.D., and Waterman, C.M. (2015). Inverted formin 2 in focal adhesions promotes dorsal stress fiber and fibrillar adhesion formation to drive extracellular matrix assembly. Proc. Natl. Acad. Sci. USA *112*, E2447–E2456.
15. Koestler, S.A., Steffen, A., Nemethova, M., Winterhoff, M., Luo, N., Holleboom, J.M., Krupp, J., Jacob, S., Vinzenz, M., Schur, F., et al. (2013). Arp2/3 complex is essential for actin network treadmilling as well as for targeting of capping protein and cofilin. Mol. Biol. Cell *24*, 2861–2875.
16. Lin, J.J., Hegmann, T.E., and Lin, J.L. (1988). Differential localization of tropomyosin isoforms in cultured nonmuscle cells. J. Cell Biol. *107*, 563–572.
17. Bryce, N.S., Schevzov, G., Ferguson, V., Percival, J.M., Lin, J.J., Matsumura, F., Bamburg, J.R., Jeffrey, P.L., Hardeman, E.C., Gunning, P., and Weinberger, R.P. (2003). Specification of actin filament function and molecular composition by tropomyosin isoforms. Mol. Biol. Cell *14*, 1002–1016.

18. Hillberg, L., Zhao Rathje, L.S., Nyåkern-Meazza, M., Helfand, B., Goldman, R.D., Schutt, C.E., and Lindberg, U. (2006). Tropomyosins are present in lamellipodia of motile cells. Eur. J. Cell Biol. *85*, 399–409.
19. Schevzov, G., Whittaker, S.P., Fath, T., Lin, J.J., and Gunning, P.W. (2011). Tropomyosin isoforms and reagents. BioArchitecture *1*, 135–164.
20. Coombes, J.D., Schevzov, G., Kan, C.-Y., Petti, C., Maritz, M.F., Whittaker, S., Mackenzie, K.L., and Gunning, P.W. (2015). Ras transformation overrides a proliferation defect induced by Tpm3.1 knockout. Cell. Mol. Biol. Lett. *20*, 626–646.
21. Temm-Grove, C.J., Jockusch, B.M., Weinberger, R.P., Schevzov, G., and Helfman, D.M. (1998). Distinct localizations of tropomyosin isoforms in LLC-PK1 epithelial cells suggests specialized function at cell-cell adhesions. Cell Motil. Cytoskeleton *40*, 393–407.
22. Schevzov, G., Vrhovski, B., Bryce, N.S., Elmir, S., Qiu, M.R., O'neill, G.M., Yang, N., Verrills, N.M., Kavallaris, M., and Gunning, P.W. (2005). Tissue-specific tropomyosin isoform composition. J. Histochem. Cytochem. *53*, 557–570.
23. Kis-Bicskei, N., Vig, A., Nyitrai, M., Bugyi, B., and Talián, G.C. (2013). Purification of tropomyosin Br-3 and 5NM1 and characterization of their interactions with actin. Cytoskeleton *70*, 755–765.
24. Lim, J.I., Sabouri-Ghomi, M., Machacek, M., Waterman, C.M., and Danuser, G. (2010). Protrusion and actin assembly are coupled to the organization of lamellar contractile structures. Exp. Cell Res. *316*, 2027–2041.
25. Wu, C., Asokan, S.B., Berginski, M.E., Haynes, E.M., Sharpless, N.E., Griffith, J.D., Gomez, S.M., and Bear, J.E. (2012). Arp2/3 is critical for lamellipodia and response to extracellular matrix cues but is dispensable for chemotaxis. Cell *148*, 973–987.
26. Dawe, H.R., Minamide, L.S., Bamburg, J.R., and Cramer, L.P. (2003). ADF/cofilin controls cell polarity during fibroblast migration. Curr. Biol. *13*, 252–257.
27. Svitkina, T.M., Verkhovsky, A.B., McQuade, K.M., and Borisy, G.G. (1997). Analysis of the actin-myosin II system in fish epidermal keratocytes: mechanism of cell body translocation. J. Cell Biol. *139*, 397–415.
28. Svitkina, T.M., and Borisy, G.G. (1999). Arp2/3 complex and actin depolymerizing factor/cofilin in dendritic organization and treadmilling of actin filament array in lamellipodia. J. Cell Biol. *145*, 1009–1026.
29. Vallotton, P., and Small, J.V. (2009). Shifting views on the leading role of the lamellipodium in cell migration: speckle tracking revisited. J. Cell Sci. *122*, 1955–1958.
30. Urban, E., Jacob, S., Nemethova, M., Resch, G.P., and Small, J.V. (2010). Electron tomography reveals unbranched networks of actin filaments in lamellipodia. Nat. Cell Biol. *12*, 429–435.
31. Vinzenz, M., Nemethova, M., Schur, F., Mueller, J., Narita, A., Urban, E., Winkler, C., Schmeiser, C., Koestler, S.A., Rottner, K., et al. (2012). Actin branching in the initiation and maintenance of lamellipodia. J. Cell Sci. *125*, 2775–2785.
32. Small, J.V. (2015). Pushing with actin: from cells to pathogens. Biochem. Soc. Trans. *43*, 84–91.
33. Liu, Z., Yang, X., Chen, C., Liu, B., Ren, B., Wang, L., Zhao, K., Yu, S., and Ming, H. (2013). Expression of the Arp2/3 complex in human gliomas and its role in the migration and invasion of glioma cells. Oncol. Rep. *30*, 2127–2136.
34. Nolen, B.J., Tomasevic, N., Russell, A., Pierce, D.W., Jia, Z., McCormick, C.D., Hartman, J., Sakowicz, R., and Pollard, T.D. (2009). Characterization of two classes of small molecule inhibitors of Arp2/3 complex. Nature *460*, 1031–1034.
35. Bailly, M., Macaluso, F., Cammer, M., Chan, A., Segall, J.E., and Condeelis, J.S. (1999). Relationship between Arp2/3 complex and the barbed ends of actin filaments at the leading edge of carcinoma cells after epidermal growth factor stimulation. J. Cell Biol. *145*, 331–345.
36. Kee, A.J., Yang, L., Lucas, C.A., Greenberg, M.J., Martel, N., Leong, G.M., Hughes, W.E., Cooney, G.J., James, D.E., Ostap, E.M., et al. (2015). An actin filament population defined by the tropomyosin Tpm3.1 regulates glucose uptake. Traffic *16*, 691–711.
37. Tojkander, S., Gateva, G., Schevzov, G., Hotulainen, P., Naumanen, P., Martin, C., Gunning, P.W., and Lappalainen, P. (2011). A molecular pathway for myosin II recruitment to stress fibers. Curr. Biol. *21*, 539–550.
38. Gunning, P.W., Hardeman, E.C., Lappalainen, P., and Mulvihill, D.P. (2015). Tropomyosin - master regulator of actin filament function in the cytoskeleton. J. Cell Sci. *128*, 2965–2974.
39. Martin, C., and Gunning, P. (2008). Isoform sorting of tropomyosins. Adv. Exp. Med. Biol. *644*, 187–200.